Inorganic Chemistry

Article

pubs.acs.org/IC

Stepwise Formation of Iridium(III) Complexes with Monocyclometalating and Dicyclometalating Phosphorus Chelates†

Cheng-Huei Lin,[†] Chih-Yuan Lin,[†] Jui-Yi Hung,[†] Yao-Yuan Chang,[†] Yun Chi,*[,†] Min-Wen Chung,[‡] Yuh-Chia Chang,[‡] Chun Liu,[‡] Hsiao-An Pan,[‡] Gene-Hsiang Lee,[‡] and Pi-Tai Chou*[,‡]

[†]Department of Chemistry, National Tsing Hua University, Hsinchu 300, Taiwan

[‡]Department of Chemistry, National Taiwan University, Taipei 106, Taiwan

Supporting Information

ABSTRACT: With the motivation of assembling cyclometalated complexes without nitrogen-containing heterocycle, we report here the design and systematic synthesis of a class of Ir(III) metal complexes functionalized with facially coordinated phosphite (or phosphonite) dicyclometalate tripod, together with a variety of phosphine, chelating diphosphine, or even monocyclometalate phosphite ancillaries. Thus, treatment of $[IrCl_3(tht)_3]$ with stoichiometric amount of triphenylphosphite (or diphenyl phenylphosphonite), two equiv of PPh_3, and in presence of NaOAc as cyclometalation promoter, gives formation of respective tripodal dicyclometalating complexes $[Ir(tpit)(PPh_3)_2Cl]$ (**2a**), $[Ir(dppit)(PPh_3)_2Cl]$ (**2b**), and $[Ir(dppit)(PMe_2Ph)_2Cl]$ (**2c**) in high yields, where $tpitH_2$ = triphenylphosphite and $dppitH_2$ = diphenyl phenylphosphonite. The reaction sequence that afforded these complexes is established. Of particular interest is isolation of an intermediate $[Ir(tpitH)(PPh_3)_2Cl_2]$ (**1a**) with monocyclometalated phosphite, together with the formation of $[Ir(tpit)(tpitH)(PPh_3)]$ (**3a**) with all tripodal, bidentate, and monodentate phosphorus donors coexisting on the coordination sphere, upon treatment of **2a** with a second equiv of triphenylphosphite. Spectroscopic studies were performed to explore the photophysical properties. For all titled Ir(III) complexes, virtually no emission can be observed in either solution at room temperature or 77 K CH_2Cl_2 matrix. Time-dependent DFT calculation indicates that the lowest energy triplet manifold involves substantial amount of metal centered ^{3}MC *dd* contribution. Due to its repulsive potential energy surface (PES) that touches the PES of ground state, the ^{3}MC *dd* state executes predominant nonradiative deactivation process.

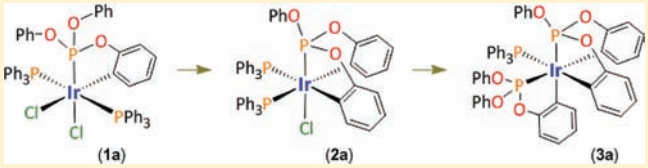

1. INTRODUCTION

Bidentate ligands such as 2,2′-bipyridine or relevant diimine chelate play an important role in the development of classical coordination chemistry, catalytic reactions, and modern material chemistry employing transition-metal based compounds.[1] However, 2,2′-bypyridine is a neutral chelate, so that it solely relies on the nitrogen-to-metal dative bonding to stabilize the resulting metal complexes. For the purpose of design and synthesis of more robust metal complexes, it is preferable to select cyclometalating chelates; thus, in addition to the nitrogen−metal dative bonding, it allows formation of carbon-to-metal covalent interaction and in turn provides the necessary stability. As a result, 2-phenyl pyridine and its functionalized analogues have been selected as the best ligands for synthesizing cyclometalates complexes.[2] Alternatively, cyclometalation also widely occurred at a variety of complexes involving late transition-metal elements.[3] Indeed, the growth of the cyclometalation compounds stimulates many studies aimed at elucidation of the mechanistic pathway or at how to widen the reaction scopes.[4] Interested readers can consult the relevant articles[2−4] for the necessary information.

Similar to the nitrogen-containing cyclometalate, the metal−phosphine coordination also allows a suitable geometrical arrangement that favors subsequent C−H activation at the nearby aromatic pendant.[5] In the case of benzyldiphenylphosphine and its functionalized derivatives, selective formation of five-membered metallacycles occurs at the benzyl site, hence it is feasible to form stable five-membered metal−chelate bonding (Scheme 1). In general, these C and P coordinated chelates also represent a class of "non-conjugated" ancillary chelates,[6] for which the cyclometalate aromatic entity and PPh_2 group are separated by a methylene group. Both fragments show stronger ligand-field strength and are capable of destabilizing the metal-centered *dd* excited states concurrently. As anticipated, after incorporating additional chromophores with desired ligand-centered $\pi\pi^*$ energy gap, decent blue to true-blue phosphor-

Scheme 1. Schematic Diagram for Benzyldiphenylphosphine Cyclometalation

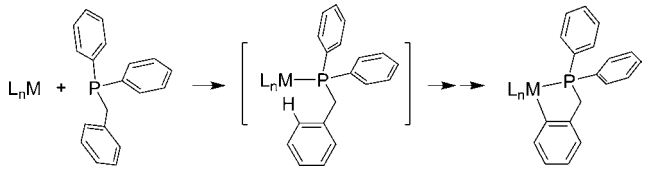

Received: September 26, 2011
Published: January 24, 2012

   dx.doi.org/10.1021/ic202090j | *Inorg. Chem.* 2012, 51, 1785−1795

escent metal complexes can be realized via tailored synthetic protocols.[7]

Another class of phosphorus donors is triphenylphosphite $P(OPh)_3$ and diphenyl phenylphosphonite $PPh(OPh)_2$, for which the phenoxy groups are capable of undergoing facile cyclometalation and affording the respective M(P∧C_2) tripodal fragment. Bearing such expectation in mind, we then carry out the reactions of Ir(III) metal reagent $[IrCl_3(tht)_3]$ with a mixture of phosphine and phosphite (or phosphonite). The well controlled reaction stoichiometry is expected to induce double cyclometalation on the phosphite (or phosphonite) ligand and afford the anticipated tripodal P∧C_2 chelating arrangement. Thus, the resulting *facial* tripod is different from that of the well-known pincer chelate of the types P^C^P and

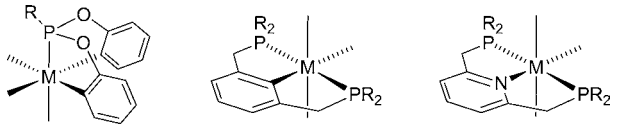

(P^C_2) (P^C^P) (P^N^P)

P^N^P, for which only the *meridional* bonding mode is reported.[8]

2. EXPERIMENTAL SECTION

General Procedures. All reactions were performed under argon atmosphere and solvents were distilled from appropriate drying agents prior to use. Commercially available reagents were used without further purification unless otherwise stated. All reactions were monitored using precoated TLC plates (0.20-mm with fluorescent indicator UV254). Mass spectra were obtained on a JEOL SX-102A instrument operating in electron impact (EI) or fast atom bombardment (FAB) mode. ^1H and ^{13}C NMR spectra were recorded on a Varian Mercury-400 or an INOVA-500 instrument. Elemental analysis was carried out with a Heraeus CHN-O Rapid Elementary Analyzer. Diphenyl phenylphosphonite ($dppitH_2$)[9] and $[IrCl_3(tht)_3]$[10] were synthesized using methods reported in the literature.

Synthesis of [Ir(tpitH)(PPh_3)$_2$$Cl_2$] (1a). $[IrCl_3(tht)_3]$ (110 mg, 0.20 mmol), triphenylphosphite ($tpitH_2$, 70 mg, 0.22 mmol), and triphenyl phosphine (PPh_3, 115 mg, 0.44 mmol) were added into 10 mL of decalin and the mixture was heated to 180 °C for 12 h. After cooling to RT, the solution was concentrated and mixed with excess of hexane to induce precipitation. The white crystals of **1a** were obtained by slow diffusion of hexane into a CH_2Cl_2 solution at RT (153 mg, 0.14 mmol, 70%).

Spectral Data of 1a. MS (FAB, ^{35}Cl, ^{193}Ir): m/z 1061 $(M - Cl)^+$. ^1H NMR (400 MHz, $CDCl_3$, 294 K): δ 7.60−7.64 (m, 12H), 7.10 (t, J = 7.4 Hz, 6H), 7.00 (t, J = 7.6 Hz, 12H), 6.94−6.84 (m, 6H), 6.71 (d, J = 8.0 Hz, 1H), 6.64 (t, J = 7.4 Hz, 1H), 6.53 (d, J = 8.0 Hz, 4H), 6.49 (d, J = 8.0 Hz, 1H), 6.02 (t, J = 7.4 Hz, 1H). $^{31}P-\{^1H\}$ NMR (202 MHz, $CDCl_3$, 294 K): δ 76.6 (t, J = 22.5 Hz, 1P), −12.8 (d, J = 22.5 Hz, 2P). Anal. Calcd for $C_{54}H_{44}Cl_2IrO_3P_3$: C, 59.12; H, 4.04. Found: C, 58.43; H, 3.89.

Synthesis of [Ir(tpit)(PPh_3)$_2$Cl] (2a). $[IrCl_3(tht)_3]$ (110 mg, 0.20 mmol), triphenylphosphite (70 mg, 0.22 mmol), and PPh_3 (115 mg, 0.44 mmol) were added into 10 mL of decalin and the mixture was heated to 180 °C for 12 h. After cooling to RT, sodium acetate (80 mg, 1.00 mmol) was added and the mixture was heated to 135 °C for another 4 h. After cooling to RT and removal of solvent, the residue was purified by silica gel column chromatography, eluting with 1:3 mixture of ethyl acetate and hexane. The white crystals of **2a** were obtained by slow diffusion of hexane into CH_2Cl_2 solution at RT (138 mg, 0.13 mmol, 65%).

Spectral Data of 2a. MS (FAB, ^{35}Cl, ^{193}Ir): m/z 1061 $(M + 1)^+$. ^1H NMR (500 MHz, $CDCl_3$, 294 K): δ 7.63 (dd, J = 7.0, 2.5 Hz, 2H), 7.35−7.32 (m, 14H), 7.19 (t, J = 6.5 Hz, 7H), 7.03 (t, J = 7.0 Hz, 12H), 6.97 (d, J = 8.5 Hz, 2H), 6.51 (t, J = 7.5 Hz, 2H), 6.42 (t, J = 7.5 Hz, 2H), 6.32 (d, J = 7.5 Hz, 2H). $^{31}P-\{^1H\}$ NMR (202 MHz, $CDCl_3$, 294 K): δ 116.3 (t, J = 13.0 Hz, 1P), −8.8 (d, J = 13.0 Hz, 2P). Anal. Calcd for $C_{54}H_{43}ClIrO_3P_3$: C, 59.12; H, 4.04. Found: C, 61.16; H, 4.09.

Synthesis of [Ir(dppit)(PPh_3)$_2$Cl] (2b). $[IrCl_3(tht)_3]$ (200 mg, 0.36 mmol), diphenyl phenylphosphonite ($dppitH_2$, 120 mg, 0.40 mmol), and PPh_3 (200 mg, 0.76 mmol) were added to 10 mL of degassed decalin and the mixture was heated to 180 °C for 12 h. After cooling to RT, sodium acetate (100 mg, 1.22 mmol) was added and the mixture was heated to 135 °C for another 4 h. After cooling to RT and removal of solvent, the residue was purified by silica gel column chromatography, eluting with 1:3 mixture of ethyl acetate and hexane. The white crystals of **2b** were obtained by slow diffusion of hexane into CH_2Cl_2 solution at RT (130 mg, 0.12 mmol, 35%).

Spectral Data of 2b. MS (FAB, ^{35}Cl, ^{193}Ir): m/z 1045 $(M + 1)^+$. ^1H NMR (500 MHz, CD_2Cl_2, 294 K): δ 7.64 (d, J = 5.5 Hz, 2H), 7.30−7.18 (m, 19H), 7.06−6.90 (m, 14H), 6.89 (td, J = 7.5, 3.5 Hz, 2H), 6.55 (t, J = 7.5 Hz, 2H), 6.45 (d, J = 7.5 Hz, 2H), 6.40 (t, J = 7.5 Hz, 2H). $^{31}P-\{^1H\}$ NMR (202 MHz, CD_2Cl_2, 294 K): δ 144.4 (t, J = 4.8 Hz, 1P), −9.8 (d, J = 4.8 Hz, 2P). Anal. Calcd for $C_{54}H_{43}ClIrO_2P_3$: C, 62.09; H, 4.15. Found: C, 61.85; H, 4.43.

Synthesis of [Ir(dppit)(PMe_2Ph)$_2$Cl] (2c). $[IrCl_3(tht)_3]$ (150 mg, 0.27 mmol), $dppitH_2$ (87 mg, 0.29 mmol), PMe_2Ph (81 mg, 0.59 mmol), and sodium acetate (110 mg, 1.35 mmol) were combined in degassed decalin (10 mL) and the mixture was heated to 180 °C for 30 h. After cooling to RT and removal of solvent, the residue was purified by silica gel column chromatography, eluting with a 1:3 mixture of ethyl acetate and hexane. The white crystals of **2c** were obtained by slow diffusion of hexane into a CH_2Cl_2 solution at RT (121 mg, 0.15 mmol, 57%).

Spectral Data of 2c. MS (FAB, ^{35}Cl, ^{193}Ir): m/z 796 $(M)^+$. ^1H NMR (500 MHz, CD_2Cl_2, 294 K): δ 8.03 (dd, J = 7.0, 3.0 Hz, 2H), 7.52 (td, J = 7.0, 1.0 Hz, 1H), 7.32 (t, J = 7.5 Hz, 2H), 7.25 (td, J = 8.0, 3.5 Hz, 2H), 7.16 (t, J = 7.0 Hz, 4H), 6.99 (dd, J = 12.0, 7.5 Hz, 2H), 6.93−6.91 (m, 4H), 6.88−6.84 (m, 2H), 6.79 (t, J = 8.0 Hz, 4H), 1.42 (d, J = 8.5 Hz, 6H), 1.10 (d, J = 9.0 Hz, 6H). $^{31}P-\{^1H\}$ NMR (202 MHz, CD_2Cl_2, 294 K): δ 141.3 (t, J = 4.8 Hz, 1P), −42.6 (d, J = 4.8 Hz, 2P). Anal. Calcd for $C_{34}H_{35}ClIrO_2P_3$: C, 51.29; H, 4.43. Found: C, 51.08; H, 4.54.

Synthesis of [Ir(tpit)(tpitH)(PPh_3)] (3a). Complex **2a** (69 mg, 0.07 mmol), triphenylphosphite (22 mg, 0.07 mmol), and sodium acetate (12 mg, 0.15 mmol) were added to 10 mL of decalin and the mixture was heated to 120 °C for 6 h. After cooling to RT and removal of solvent, the residue was purified by silica gel column chromatography, eluting with a 4:1 mixture of dichloromethane and hexane. The white crystals of **3a** were obtained by slow diffusion of hexane into CH_2Cl_2 solution at RT (54 mg, 0.05 mmol, 77%).

Spectral Data of 3a. MS (FAB, ^{193}Ir): m/z 1072 $(M)^+$. ^1H NMR (500 MHz, CD_2Cl_2, 294 K): δ 7.48 (t, J = 8.0 Hz, 1H), 7.35 (t, J = 8.0 Hz, 2H), 7.26−7.20 (m, 5H), 7.19−7.15 (m, 4H), 7.11 (dd, J = 8.0, 3.0 Hz, 1H), 7.06−7.04 (m, 15H), 6.97 (d, J = 8.5 Hz, 2H), 6.77−6.73 (m, 4H), 6.70 (t, J = 7.5 Hz, 1H), 6.60−6.55 (m, 5H), 6.51 (t, J = 7.5 Hz, 1H), 6.21 (dd, J = 8.0, 3.0 Hz, 1H). $^{31}P-\{^1H\}$ NMR (202 MHz, CD_2Cl_2, 294 K): δ 141.8 (dd, J = 20.0, 12.1 Hz, 1P), 114.5 (dd, J = 20.0, 12.1 Hz, 1P), −4.1 (t, J = 20.0 Hz, 1P). Anal. Calcd for $C_{54}H_{42}IrO_6P_3$: C, 60.50; H, 3.95. Found: C, 60.33; H, 4.02.

Synthesis of [Ir(tpit)(dppb)Cl] (4a). Complex **2a** (100 mg, 0.10 mmol) and 1,2-bis(diphenylphosphino)benzene (dppb, 47 mg, 0.11 mmol) were added to 10 mL of decalin and the mixture was heated to 110 °C for 2 h. After cooling to RT and removal of solvent, the residue was purified by silica gel column chromatography, eluting with a 4:1 mixture of dichloromethane and hexane. The white crystals of **4a** were obtained by slow diffusion of hexane into CH_2Cl_2 solution at RT (77 mg, 0.08 mmol, 83%).

Spectral Data of 4a. MS (FAB, ^{35}Cl, ^{193}Ir): m/z 983 $(M + 1)^+$. ^1H NMR (400 MHz, $CDCl_3$, 294 K): δ 7.65−7.54 (m, 10H), 7.37−7.29 (m, 2H), 7.28−7.20 (m, 4H), 7.18−7.09 (m, 8H), 7.08−6.95 (m, 5H), 6.84−6.75 (m, 4H), 6.65 (t, J = 8.0 Hz, 2H), 6.33 (d, J = 8.0 Hz, 2H).

dx.doi.org/10.1021/ic202090j | Inorg. Chem. 2012, 51, 1785−1795

Table 1. Crystal Data and Refinement Parameters for Complexes 1a, 2a, 2c, 3a, 4b, and 5b

	1a	2a	2c	3a	4b	5b
empirical formula	$C_{44}H_{36.80}Cl_{3.20}Ir_{0.80}O_{2.40}P_{2.40}$	$C_{55}H_{45}Cl_3IrO_3P_3$	$C_{34}H_{35}ClIrO_2P_3$	$C_{54}H_{42}IrO_6P_3$	$C_{49}H_{39}Cl_3IrO_2P_3$	$C_{49}H_{37}IrNO_2P_3S$
formula weight	945.46	1145.37	796.18	1071.99	1051.26	988.97
temperature, K	150(2)	150(2)	150(2)	150(2)	150(2)	150(2)
crystal system	monoclinic	triclinic	monoclinic	triclinic	monoclinic	orthorhombic
space group	$P2_1/c$	$P\bar{1}$	$P2_1/n$	$P\bar{1}$	$P2_1/n$	$Pbca$
a, Å	13.0584(6)	11.7548(5)	9.8586(6)	11.8016(2)	10.9011(7)	20.2319(10)
b, Å	12.6063(6)	13.1516(6)	19.3800(11)	12.3056(3)	22.1877(14)	19.0994(9)
c, Å	31.5539(16)	16.9951(8)	16.0905(9)	16.2714(4)	17.7327(11)	20.9480(11)
α, °		85.774(1)		81.0150(9)		
β, °	99.463(1)	70.345(1)	94.5344(12)	82.7381(12)	91.5227(13)	
γ, °		69.699(1)		70.8637(9)		
volume, Å^3	5123.7(4)	2317.82(18)	3064.6(3)	2197.88(8)	4287.5(5)	8094.7(7)
Z	5	2	4	2	4	8
ρ_{calcd}, Mg m^{-3}	1.532	1.641	1.726	1.620	1.629	1.623
absorption coefficient, mm^{-1}	2.951	3.203	4.632	3.201	3.453	3.512
$F(000)$	2360	1144	1576	1072	2088	3936
crystal size, mm^3	0.43 × 0.20 × 0.20	0.27 × 0.25 × 0.15	0.25 × 0.20 × 0.15	0.18 × 0.14 × 0.13	0.27 × 0.18 × 0.10	0.36 × 0.18 × 0.10
reflections collected	35231	23947	23464	38394	32679	60149
independent reflections	11737 [R(int) = 0.0377]	10588 [R(int) = 0.0311]	7038 [R(int) = 0.0298]	10067 [R(int) = 0.0554]	9834 [R(int) = 0.0341]	9301 [R(int) = 0.0559]
max., min transmission	0.5898, 0.3635	0.6451, 0.4784	0.5434, 0.3906	0.639, 0.579	0.7239, 0.4557	0.7203, 0.3646
data/restraints/parameters	11737/5/587	10588/0/586	7038/0/374	10067/0/577	9834/0/523	9301/1/514
goodness-of-fit on F^2	1.095	1.072	1.124	1.020	1.088	1.025
final R indices [$I > 2\sigma(I)$]	R_1 = 0.0404, wR_2 = 0.1056	R_1 = 0.0299, wR_2 = 0.0692	R_1 = 0.0255, wR_2 = 0.0538	R_1 = 0.0326, wR_2 =0.0648	R_1 = 0.0285, wR_2 = 0.0626	R_1 = 0.0261, wR_2 = 0.0584
R indices (all data)	R_1 = 0.0501, wR_2 = 0.1122	R_1 = 0.0341, wR_2 = 0.0767	R_1 = 0.0279, wR_2 = 0.0547	R_1 = 0.0489, wR_2 = 0.0746	R_1 = 0.0331, wR_2 = 0.0644	R_1 = 0.0355, wR_2 = 0.0632
largest different peak and hole	1.862 and −1.046 e.Å^{-3}	1.369 and −0.815 e.Å^{-3}	1.186 and −0.736 e.Å^{-3}	1.209 and −1.677 e.Å^{-3}	1.220 and −0.889 e.Å^{-3}	1.254 and −1.148 e.Å^{-3}

$^{31}P-\{^1H\}$ NMR (202 MHz, $CDCl_3$, 294 K): δ 117.3 (t, J = 9.9 Hz, 1P), 16.0 (d, J = 9.9 Hz, 2P). Anal. Calcd for $C_{48}H_{37}ClIrO_3P_3$: C, 58.68; H, 3.80. Found: C, 58.54; H, 4.05.

Synthesis of [Ir(dppit)(dppb)Cl] (4b). Complex **4b** was prepared from **2b** using a procedure similar to that for **4a**; yield: 95%.

Spectral Data of 4b. MS (FAB, ^{35}Cl, ^{193}Ir): m/z 967 (M + 1)$^+$. ^1H NMR (400 MHz, $CDCl_3$, 294 K): δ 7.83−7.77 (m, 2H), 7.72−7.65 (m, 2H), 7.42 (t, J = 8.0 Hz, 2H), 7.35−7.23 (m, 7H), 7.15 (t, J = 8.0 Hz, 4H), 7.01−6.89 (m, 12H), 6.82 (t, J = 8.0 Hz, 2H), 6.59−6.50 (m, 4H), 6.25 (d, J = 8.0, 1H), 6.22 (d, J = 8.0, 1H). $^{31}P-\{^1H\}$ NMR (202 MHz, $CDCl_3$, 294 K): δ 149.9 (t, J = 2.6 Hz, 1P), 16.6 (d, J = 2.6 Hz, 2P). Anal. Calcd for $C_{48}H_{37}ClIrO_2P_3$: C, 59.66; H, 3.86. Found: C, 58.70; H, 4.22.

Synthesis of [Ir(tpit)(dppb)(NCS)] (5a). Complex **4a** (50 mg, 0.05 mmol) and potassium thiocyanate (50 mg, 0.51 mmol) were added in 10 mL of DMF (10 mL) and the mixture was refluxed for 36 h. After cooling to RT and removal of solvent, the residue was purified by silica gel column chromatography, eluting with a 4:1 mixture of dichloromethane and hexane. The white crystals of **5a** were obtained by slow diffusion of hexane into CH_2Cl_2 solution at RT (36 mg, 0.04 mmol, 70%).

Spectral data of 5a. MS (FAB, ^{193}Ir): m/z 1005 (M)$^+$. ^1H NMR (400 MHz, $CDCl_3$, 294 K): δ 7.67−7.63 (m, 4H), 7.46−7.33 (m, 12H), 7.29−7.25 (m, 2H), 7.19−7.12 (m, 6H), 7.07 (t, J = 6.0 Hz, 1H), 6.97 (t, J = 8.0 Hz, 4H), 6.82 (t, J = 6.0 Hz, 2H), 6.71 (t, J = 6.0 Hz, 2H), 6.63 (d, J = 8.0 Hz, 2H), 6.31 (d, J = 8.0 Hz, 2H). $^{31}P-\{^1H\}$ NMR (202 MHz, $CDCl_3$, 294 K): δ 117.3 (br, 1P), 17.22 (d, J = 14.9 Hz, 2P). Anal. Calcd for $C_{49}H_{37}IrNO_3P_3S$: C, 58.56; H, 3.71; N, 1.39. Found: C, 58.41; H, 3.98; N, 1.41.

Synthesis of [Ir(dppit)(dppb)(NCS)] (5b). Complex **5b** was prepared from **4b** using a procedure similar to that for **5a**; yield: 85%.

Spectral Data of 5b. MS (FAB, ^{193}Ir): m/z 990 (M + 1)$^+$. ^1H NMR (400 MHz, $CDCl_3$, 294 K): δ 7.77−7.74 (m, 2H), 7.69−7.67 (m, 2H), 7.39−7.30 (m, 6H), 7.15−7.09 (m, 8H), 7.07−7.00(m, 5H), 6.93−6.86 (m, 8H), 6.63−6.58 (m, 4H), 6.12 (d, J = 8.0 Hz, 1H), 6.09 (d, J = 8.0 Hz, 1H). $^{31}P-\{^1H\}$ NMR (202 MHz, $CDCl_3$, 294 K): δ 146.0 (br, 1P), 17.3 (d, J = 3.8 Hz, 2P). Anal. Calcd for $C_{49}H_{37}IrNO_2P_3S$: C, 59.51; H, 3.77; N, 1.42. Found: C, 59.45; H, 3.99; N, 1.81.

Synthesis of [Ir(dppit)(PMe$_2$Ph)$_2$(NCS)] (6c). Complex **6c** was prepared from **2b** using a procedure similar to that for **5a**; yield: 64%.

Spectral Data of 6c. MS (FAB, ^{193}Ir): m/z 820 (M + 1). ^1H NMR (400 MHz, CD_3Cl, 294 K): δ 7.75−7.70 (m, 2H), 7.57 (t, J = 8.0 Hz, 1H), 7.36−7.30 (m, 4H), 7.18−7.14 (m, 6H), 6.93−6.88 (m, 6H), 6.76 (t, J = 8.0 Hz, 4H), 1.42 (d, J = 8.0 Hz, 6H), 1.13 (d, J = 8.0 Hz, 6H). $^{31}P-\{^1H\}$ NMR (202 MHz, $CDCl_3$, 294 K): δ 139.7 (br, 1P), −39.8 (d, J = 7.5 Hz, 2P). Anal. Calcd for $C_{35}H_{35}IrNO_2P_3S$: C, 51.34; H, 4.31; N, 1.71. Found: C, 51.02; H, 4.65; N, 1.80.

Single Crystal X-ray Diffraction Studies. Single crystal X-ray diffraction data were measured on a Bruker SMART Apex CCD diffractometer using (Mo Kα) radiation (λ = 0.71073 Å). The data collection was executed using the SMART program. Cell refinement and data reduction were performed with the SAINT program. The structure was determined using the SHELXTL/PC program and refined using full-matrix least-squares. All crystallographic data and refinement parameters are summarized in Table 1.

Photophysical Investigation and Theoretical Methodology. Steady-state absorption, emission, and phosphorescence lifetime measurements in solution and solid state have been described in our previous reports.[11] Calculations on electronic singlet and triplet states of all titled complexes were carried out using the density functional theory (DFT) with B3LYP hybrid functional.[12] Restricted and unrestricted formalisms were adopted in the singlet and triplet

dx.doi.org/10.1021/ic202090j | Inorg. Chem. 2012, 51, 1785−1795

geometry optimization, respectively. A "double-ζ" quality basis set consisting of Hay and Wadt's effective core potentials (LANL2DZ)[13] was employed for the Ir(III) metal atom, and a 6-31G* basis set[14] was employed for the rest of the atoms. The relativistic effective core potential (ECP) replaced the inner core electrons of Ir(III) metal atom, leaving only the outer core valence electrons ($5s^25p^65d^6$) to be concerned. Time-dependent DFT (TDDFT) calculations using the B3LYP functional were then performed based on the optimized structures at the ground state.[15] Moreover, considering the solvation effect, the calculations were then combined with an integral equation formalism-polarizable continuum model (in dichloromethane), IEF-PCM,[16] implemented in Gaussian 03. Typically, 10 lower triplet and singlet roots of the nonhermitian eigenvalue equations were obtained to determine the vertical excitation energies. Oscillator strengths were then deduced from the dipole transition matrix elements (for singlet states only). All calculations were carried out using Gaussian 03.[17]

3. RESULTS AND DISCUSSION

Stepwise Dicyclometalation. It was reported that treatment of $[IrCl_3(tht)_3]$ (tht = tetrahydrothiophene) with an equimolar amount of triphenylphosphite ($tpitH_2$) and diimine, such as 2,2′-bipyridine and 2,2′-biquinoline, gave formation of novel diimine complexes **A** and **B** (see below) in high yields.[18] The added diimine and phosphite would easily replace all three tht ligands and then formed certain unknown intermediate initially. Moreover, the phosphite coordination would also bring two of its phenyl substituents near the central Ir(III) atom and then facilitate the subsequent double cyclometalation with the assistance of sodium acetate added to the mixture. This strategy presents a synthetic protocol in obtaining a new class of emissive Ir(III) complexes without the employment of traditional nitrogen-containing polyaromatic cyclometalates.

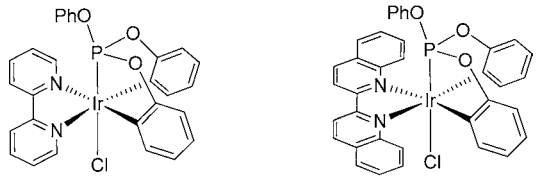

(**A**) (**B**)

Upon replacing the diimine with two equal molar ratio of PPh_3, the same reaction of $[IrCl_3(tht)_3]$ with triphenylphosphite and excess of sodium acetate in refluxing decalin solution resulted in a high yield conversion to a dicyclometalated phosphite complex $[Ir(tpit)(PPh_3)(OAc)]$ (**C**) (c.f. Scheme 2).[19] Subsequent replacement of acetate in **C** with 3-*tert*-butyl-5-(2-pyridyl) triazolate chromophoric chelate gave isolation of the blue-emitting phosphor $[Ir(tpit)(PPh_3)(bptz)]$ (**D**) in high yield (∼ 60%). Intriguingly, the complexes with relevant P^C_2 tripodal chelate were known as products from reaction of the hindered phosphites $P(OAr)_3$ (Ar = C_6H_4-2-*t*Bu or C_6H_3-2,4-tBu_2) and Ir(I) reagents $[\{Ir(\mu\text{-OMe})(cod)\}_2]$ or $[Ir(cod)(py)_2][PF_6]$, for which the steric effect is proposed to be the main driving force for the observed double cyclometalation.[20] The dicyclometalation may be favored over monocyclometalation as a means to minimize the intramolecular interaction between the *t*-Bu groups in the phosphite ligand. However, such a steric demand imposed by the bulky *t*Bu groups does not exist in our Ir(III) system. To gain more insight into the phosphite cyclometalation, we thus carry out further investigation by conducting the reaction in presence of excess triphenylphosphine to slow down the reaction sequence, so that certain intermediate species can be isolated.

Scheme 2. Synthetic Route to the Ir(III) Complexes C and D (Reagents and Conditions: (i) 190 °C, decalin, 6 h, (ii) (bptz)H, 190 °C, 12 h)

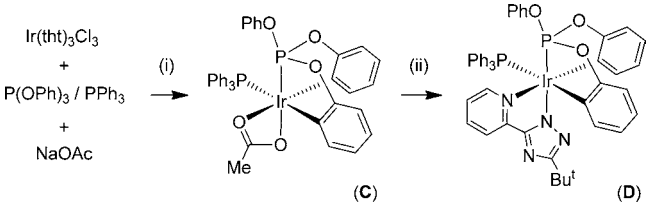

We first allowed $[IrCl_3(tht)_3]$ to react with stoichiometric amount of $P(OPh)_3$ (also denoted as $tpitH_2$) plus two equiv of PPh_3, but in absence of NaOAc. The addition of PPh_3 or other phosphorus donor is intended to prevent the formation of any vacant coordination site that would yield the chloride-bridged dimer, which is prevalent for the chloride containing Ir(III) metal complexes;[21] otherwise, severe decomposition could take place. As indicated in Scheme 3, this reaction in presence of PPh_3 afforded one major Ir(III) product $[Ir(tpitH)(PPh_3)_2Cl_2]$ (**1a**) which can be isolated via simple precipitation, followed by crystallization. The $^{31}P-\{^1H\}$ NMR spectrum shows two signals at δ 76.57 and 12.78 with intensity ratio of 1:2, showing the attachment of one phosphite and two phosphines, respectively.

Scheme 3. Synthetic Route to the Ir(III) Complexes 1a and 2a (Reagents and Conditions: (i) 180 °C, decalin, 12 h, (ii) NaOAc, 135 °C, 4 h)

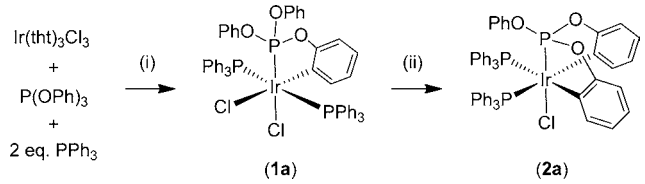

The single-crystal X-ray structures of **1a** were then determined. Figure 1 shows the ORTEP drawing, along with selected bond lengths and angles that are given in the caption. The structure is in agreement with the NMR data; in particular it is clear that the phosphite has underwent only monocyclometalation, giving a symmetrical core arrangement with two PPh_3 and two chloride ligands occupying trans and cis

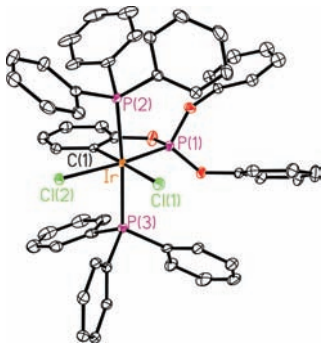

Figure 1. ORTEP diagram of **1a** with ellipsoids shown at 30% probability level. Selected bond distances: Ir–P(1) = 2.1898(12), Ir–P(3) = 2.3956(12), Ir–P(2) = 2.3968(12), Ir–C(1) = 2.079(5), Ir–Cl(2) = 2.4189(11), and Ir–Cl(1) = 2.4541(11) Å.

dx.doi.org/10.1021/ic202090j | Inorg. Chem. 2012, 51, 1785–1795

coordination sites. Furthermore, the metal−phosphite distance (Ir−P(1) = 2.1898(12) Å) is substantially shorter than that of metal−phosphine distances (Ir−P(3) = 2.3956(12) and Ir−P(2) = 2.3968(12) Å). This reflects the weaker Ir−P bonding for PPh_3, a result of greater steric demand, plus weaker π-accepting character of its phosphorus atom. Furthermore, both Ir−Cl distances are identical within the experimental error, despite the fact that they are located in quite different environments, i.e., located trans to the cyclometalated carbon and phosphorus atoms, respectively.

In an attempt to study the accompanied reactivity pattern, **1a** was then heated in decalin and in presence of NaOAc at 135 °C for 4 h. The subsequent major product $[Ir(tpit)(PPh_3)_2Cl]$ (**2a**) showed no obvious difference in color from its starting material **1a**, whereas its chemical stability had been significantly improved, as revealed by showing no visible decomposition during separation employing silica gel column chromatography. Next, the FAB analysis showed a molecular ion (M^+) at m/z 1060 which is 36 units smaller that that of **1a**, confirming the elimination of an additional HCl fragment. In good agreement with the FAB data, the $^{31}P-\{^1H\}$ spectrum recorded shows the presence of two mutually coupled multiplets at δ 116.26 and δ −8.75 (J = 13.0 Hz) with intensity ratio 1:2. Therefore, **2a** is assigned to possess the double cyclometalated structure as shown in Scheme 3. Moreover, the conversion from **1a** to **2a** required only higher reaction temperature, extended reaction time, and addition of sodium acetate (NaOAc) as the cyclometalation promoter. Direct synthesis of **2a** can then be done employing a one-pot sequence starting from $[IrCl_3(tht)_3]$ and a mixture of PPh_3, phosphate $P(OPh)_3$, and NaOAc. Moreover, switching from phosphite $P(OPh)_3$ to phosphonite $PPh(OPh)_2$ and replacing PPh_3 with PMe_2Ph gave isolation of two more functionalized derivatives **2b** and **2c**, both in excellent yields (Scheme 4). This expanded reaction scope

Scheme 4. Synthetic Route to the Ir(III) Complexes 2b and 2c (Reagents and Conditions: (i) 180 °C, decalin, 12 h)

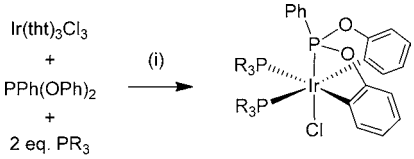

(**2b**) $PR_3 = PPh_3$
(**2c**) $PR_3 = PMe_2Ph$

then confirms the sequential mono- and dicyclometalation capability on the Ir(III) metal center, for both phosphite and phosphonite ligands demonstrated earlier.

Crystals of complexes **2a** and **2c** were grown by slow diffusion of hexane into the CH_2Cl_2 solution. The X-ray crystal structural data are in line with the spectral data just discussed, with selected bond distances and angles given in the captions of Figures 2 and 3. Their structural feature is akin to three Ir(III) complexes with facially coordinated phosphite tripod, namely hydride complexes $[IrH(cod)\{P(OC_6H_4)_2(OC_6H_5)\}]$ and $[IrH\{P(OC_6H_2\text{-}2,4\text{-}tBu_2)_2(OC_6H_3\text{-}2,4\text{-}tBu_2)\}(cod)]$ reported by Bedford,[20] and γ-picoline coordinated derivative $[IrP\{(OC_6H_3Me)_2(OC_6H_4Me)\}Cl(4Me\text{-}py)_2]$ reported by Singleton.[22] Moreover, close comparison between **2a** and **2c** shows that the phosphite Ir−P distance (2.1529(8) Å) is notably shorter than the phosphonite Ir−P distance (2.1896(8) Å), while the PMe_2Ph also shows stronger Ir−P bonding than that

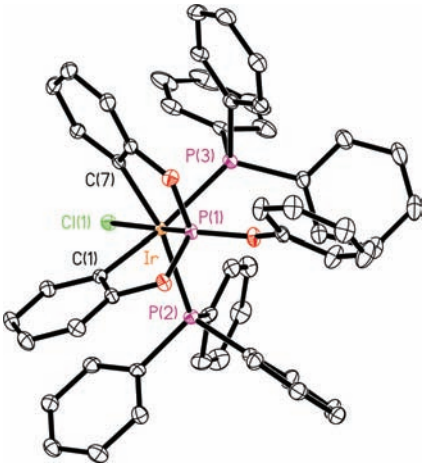

Figure 2. ORTEP diagram of **2a** with ellipsoids shown at 30% probability level. Selected bond distances: Ir−P(1) = 2.1529(8), Ir−P(3) = 2.4433(8), Ir−P(2) = 2.4528(9), Ir−C(7) = 2.081(3), Ir−C(1) = 2.103(3), and Ir−Cl(1) = 2.4385(8) Å; bond angle: P(2)−Ir-P(3) = 104.97(3)°.

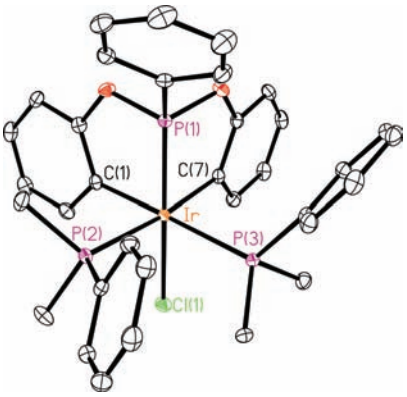

Figure 3. ORTEP diagram of **2c** with ellipsoids shown at 30% probability level. Selected bond distances: Ir−P(1) = 2.1896(8), Ir−P(2) = 2.3698(8), Ir−P(3) = 2.3812(8), Ir−Cl(1) = 2.4469(7), Ir−C(1) = 2.090(3), and Ir−C(7) = 2.104(3) Å; bond angle: P(2)−Ir−P(3) = 100.28(3)°.

of the respective PPh_3 ligands. This variation of Ir−P distances seems to be parallel to the general electronic and steric properties of phosphorus donor ligands.[23]

Additional Cyclometalation Reaction. When complex **2a** was treated with 1 equiv of $P(OPh)_3$ in presence of NaOAc, a new complex $[Ir(tpit)(tpitH)(PPh_3)]$ (**3a**) was formed after heating at 120 °C for 6 h. The $^{31}P-\{^1H\}$ NMR spectrum of **3a** exhibits three signals at δ 141.84, 114.52, and −4.11. Based on their ^{31}P NMR chemical shift data, we concluded the existence of two phosphites and one PPh_3 on the Ir(III) coordination sphere, i.e., showing the occurrence of phosphine−phosphite exchange. Further evidence is provided by the single crystal X-ray analysis shown in Figure 4. As can be seen, the Ir(III) center adopts a distorted octahedral coordination geometry, which is then coordinated by one dicyclometalated and one mono-cyclometalated phosphite, together with one remaining PPh_3. Remarkably, all three cyclometalated phenyl groups and phosphorus donor atoms are now adopting the *facial* mode, which has been considered to be the thermodynamically favorable coordination motif for a majority of Ir(III) metal complexes.[24]

dx.doi.org/10.1021/ic202090j | Inorg. Chem. 2012, 51, 1785−1795

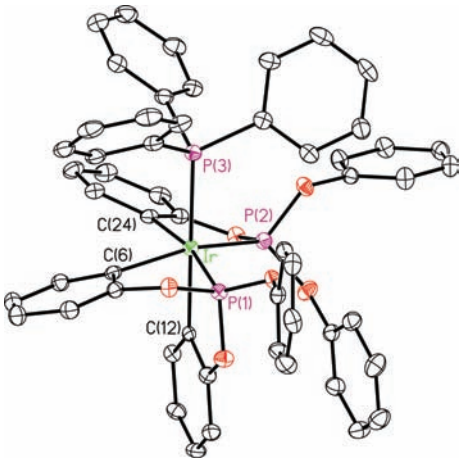

Figure 4. ORTEP diagram of **3a** with ellipsoids shown at 30% probability level. Selected bond distances: Ir–P(1) = 2.2340(9), Ir–P(2) = 2.2518(9), Ir–P(3) = 2.3940(10) Å, Ir–C(6) = 2.133(3), Ir–C(12) = 2.118(4), and Ir–C(24) = 2.126(3) Å.

Simple Ligand Substitution. Parallel to the phosphine-to-phosphite exchange that led to the cyclometalation of phosphite, replacement of PPh_3 in both **2a** and **2b** with 1,2-bis(diphenylphosphino)benzene (dppb) afforded the simple substitution products [Ir(tpit)(dppb)Cl] (**4a**) and [Ir(dppit)-(dppb)Cl] (**4b**) in good yields (Schemes 5 and 6). The greater

Scheme 5. Synthetic Route to the Ir(III) Complexes 3a–5a (Reagents and Conditions: (i) $P(OPh)_3$, NaOAc, 120 °C, decalin, 6 h, (ii) o-$C_6H_4(PPh_2)_2$, 110 °C, 2 h, (iii) KNCS, DGME, 190 °C)

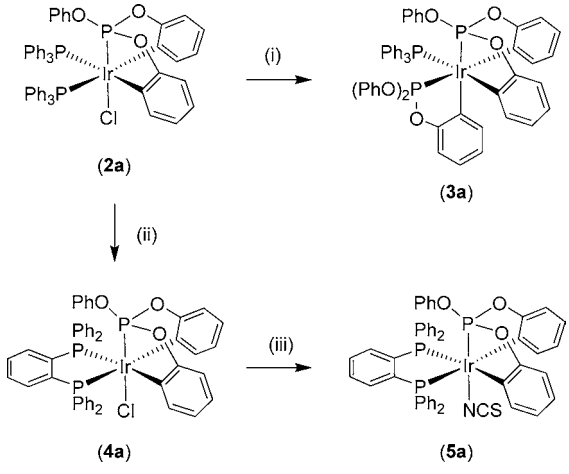

rigidity of the chelating dppb may enhance its stability against further phosphine substitution. We then made attempts to replace chloride with either phenyl or phenylacetylide fragment. These reactions were attempted by treatment of **4a** (or **4b**) with phenylmagnesium bromide in anhydrous dimethoxy-ethane or with phenylacetylene in triethylamine and in presence of CuI as catalyst. These two procedures are known to be useful for incorporation of the respective organic group into the late transition metal halide complexes;[25] however, none of them can yield the anticipated products in the current Ir(III) system. The poor reactivity could be attributed to the 3+ oxidation state of the Ir(III) atoms, which could enhance the covalent character of the Ir–Cl bonding and hence the

Scheme 6. Synthetic Route to the Ir(III) Complexes 4b, 5b, and 6c (Reagents and Conditions: (i) o-$C_6H_4(PPh_2)_2$, 110 °C, 2 h, (ii) KNCS, DMF, reflux, 24 h)

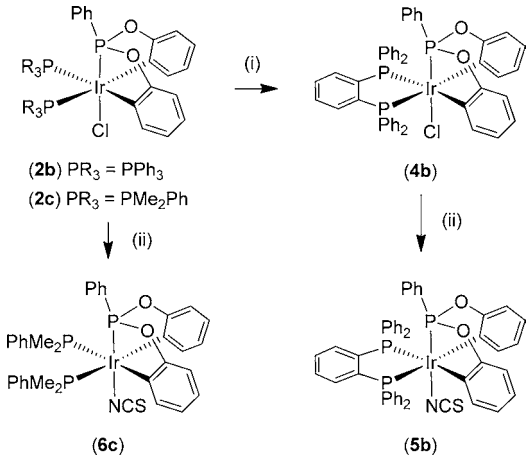

increased bond strength. In contrast, the chloride–thiocyanate exchange reaction, which gives [Ir(tpit)(dppb)(NCS)] (**5a**) and [Ir(dppit)(dppb)(NCS)] (**5b**), proceeds with better yields than that afforded the counterpart [Ir(dppit)-$(PMe_2Ph)_2$(NCS)] (**6c**), despite the fact that all of them need higher reaction temperature and extended reaction time. Evidently, the low yield in **6c** is attributed to the inferior stability of its starting material **2c**, which possesses two monodentate PMe_2Ph instead of the more robust chelating dppb existing in both **4a** and **4b**.

For confirming the bonding mode of dppb chelate, the molecular structures of both Ir(III) complexes **4b** and **5b** were determined by X-ray crystallographic analyses. Figures 5 and 6

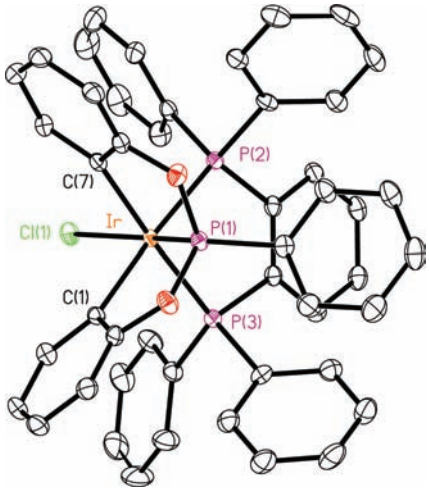

Figure 5. ORTEP diagram of **4b** with ellipsoids shown at 30% probability level. Selected bond distances: Ir–P(1) = 2.2084(8), Ir–P(2) = 2.3544(7), Ir–P(3) = 2.3478(8), Ir–Cl(1) = 2.4211(7), Ir–C(1) = 2.101(3), and Ir–C(7) = 2.108(3) Å; bond angle: P(2)–Ir–P(3) = 84.69(3)°.

show the ORTEP drawings of **4b** and **5b** with selected bond distances and angles provided in the captions. It is notable that the coordination environments around the Ir(III) metal center of **4b** and **5b** are essentially the same, and each iridium atom possesses an octahedral geometry. The bite angles of dppb for **4b** and **5b** are P(2)–Ir–P(3) = 84.69(3) and 84.68(3)°,

dx.doi.org/10.1021/ic202090j | Inorg. Chem. 2012, 51, 1785–1795

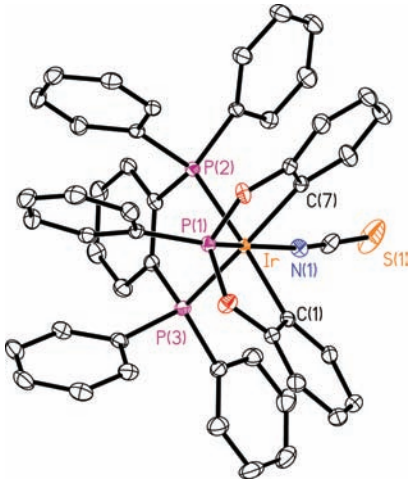

Figure 6. ORTEP diagram of **5b** with ellipsoids shown at 30% probability level. Selected bond distances: Ir–P(1) = 2.2062(7), Ir–P(2) = 2.3508(7), Ir–P(3) = 2.3611(7), Ir–N(1) = 2.072(2), Ir–C(1) = 2.113(3), and Ir–C(7) = 2.099(3) Å; bond angle: P(2)–Ir–P(3) = 84.68(3)°.

respectively, for which both are close to the ideal bite angle for undistorted octahedral metal complexes, and are much more acute than that of the P–Ir–P angle observed for **2a** and **2c** (c.f. 104.97(3) and 100.28(3)°), confirming the thermodynamical consequence of dual phosphine-to-chelating diphosphine substitution. Finally, structure of **5b** also reveals an N-coordination of thiocyanate, which is consistent with the bonding mode observed for other thiocyanate-containing metal complexes.[26]

Photophysical Properties. Figures 7 and 8 display the absorption spectra of all titled Ir(III) complexes **2a–6c**

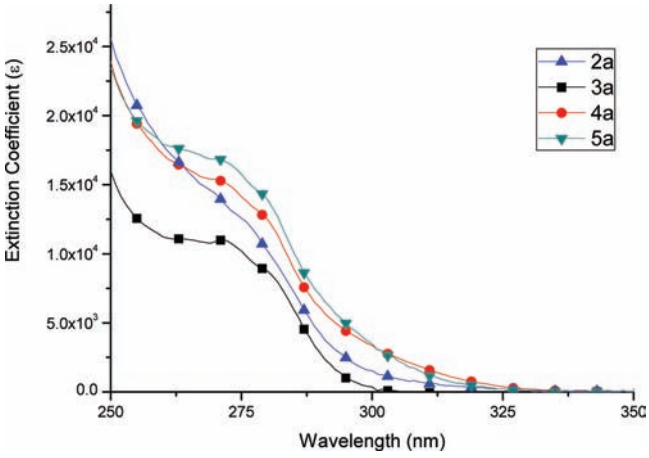

Figure 7. Absorption spectra of **2a–5a** in CH_2Cl_2 solution at room temperature (symbols as given in key).

recorded in degassed CH_2Cl_2 at room temperature. In general, all complexes exhibit allowed absorption bands in the UV region of <275 nm, for which ε values at the peak maxima are measured to be $>1.5 \times 10^4$ M^{-1} cm^{-1} and can thus be attributed to ligand-centered $\pi\pi^*$ transition. The broad band at longer wavelength up to 330 nm, as revealed by their relatively lower extinction coefficients ($<1.0 \times 10^3$ M^{-1} cm^{-1}), is assigned to the tail of $\pi\pi^*$ transition overlapping with the metal-to-ligand charge transfer (MLCT) transition and a certain extent of

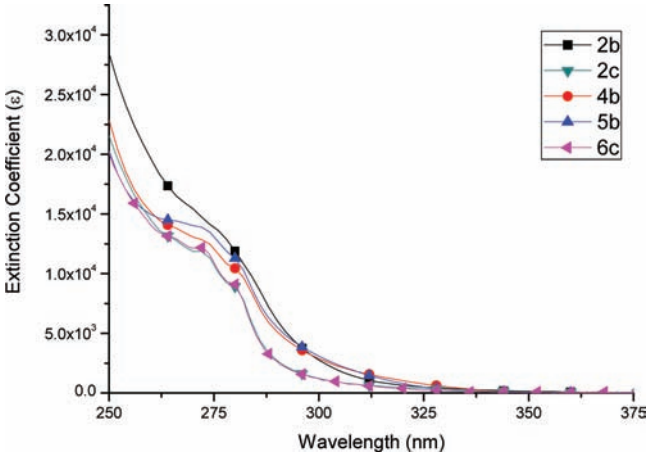

Figure 8. Absorption spectra of **2b–6c** in CH_2Cl_2 solution at room temperature (symbols as given in key).

metal-centered (MC) *dd* transition (*vide infra*) in the singlet manifold. The lower lying states all located in the UV region (< 400 nm) are predictable mainly due to the lack of π-extended, highly conjugated ligands for the titled complexes. As for the luminescence property, all titled complexes are nonemissive in degassed CH_2Cl_2 solution as well as in solid state at RT. Also, barely any emission could be resolved in the 77 K CH_2Cl_2 matrix. The lack of emission may not be unexpected, which can be attributed to the high $\pi\pi^*$ energy gap for the nonconjugated phenyl fragments associated with the Ir(III) metal atom. Such a design strategy reduces π-conjugation length significantly and thus tunes the absorption band to the UV region, at which the absorption is plausibly coupled to the MC *dd* transition that is then subject to dominant quenching via interaction between MC *dd* repulsive potential energy surface (PES) and PES of the ground state.[27]

To gain more in-depth information into the photophysical properties, time-dependent (TD) DFT was then performed via the use of functional B3LYP and the 6-31G(d)/LANL2DZ basis set. Also, the PCM model in CH_2Cl_2 is incorporated to take the solvation effect into account (see Experimental Section for detail). Figures 9 and 10 depict the selected frontier orbitals involved in lower-lying transitions of all titled complexes. The calculated energy gaps and corresponding assignments of each transition are listed in Table 2. Accordingly, the calculated $S_0 \rightarrow S_1$ transition (in terms of wavelength) of all studied complexes is close to the observed onsets of the lowest energy absorption spectra depicted in Figures 7 and 8. Taking **2a** and **2b** as examples, the computational energy gaps of the S_1 states (**2a**: 337 nm, **2b**: 362.3 nm) are qualitatively in agreement with the onset of their lowest energy absorption peak. This result indicates that the TDDFT calculation works well in predicting the lowest Franck–Condon excited state for absorption based on the S_0 optimized geometries of all Ir(III) metal complexes.

Table 2 also lists the T_1 energy gap and the frontier orbitals involved in the S_0–T_1 transition, both of which play a key role in interpreting the lack of emission under all conditions. As for the transition characteristic, frontier orbital analyses indicate that the lowest energy triplet states (T_1) for all Ir(III) complexes are primarily attributed to HOMO → LUMO transition (c.f. Table 2), mixed with transitions from lower lying HOMO-n to higher lying LUMO+m orbitals. Careful examination indicates that the T_1 state, to certain extents, always involves non-negligible amount of d_{σ^*} contribution (c.f.

dx.doi.org/10.1021/ic202090j | Inorg. Chem. 2012, 51, 1785–1795

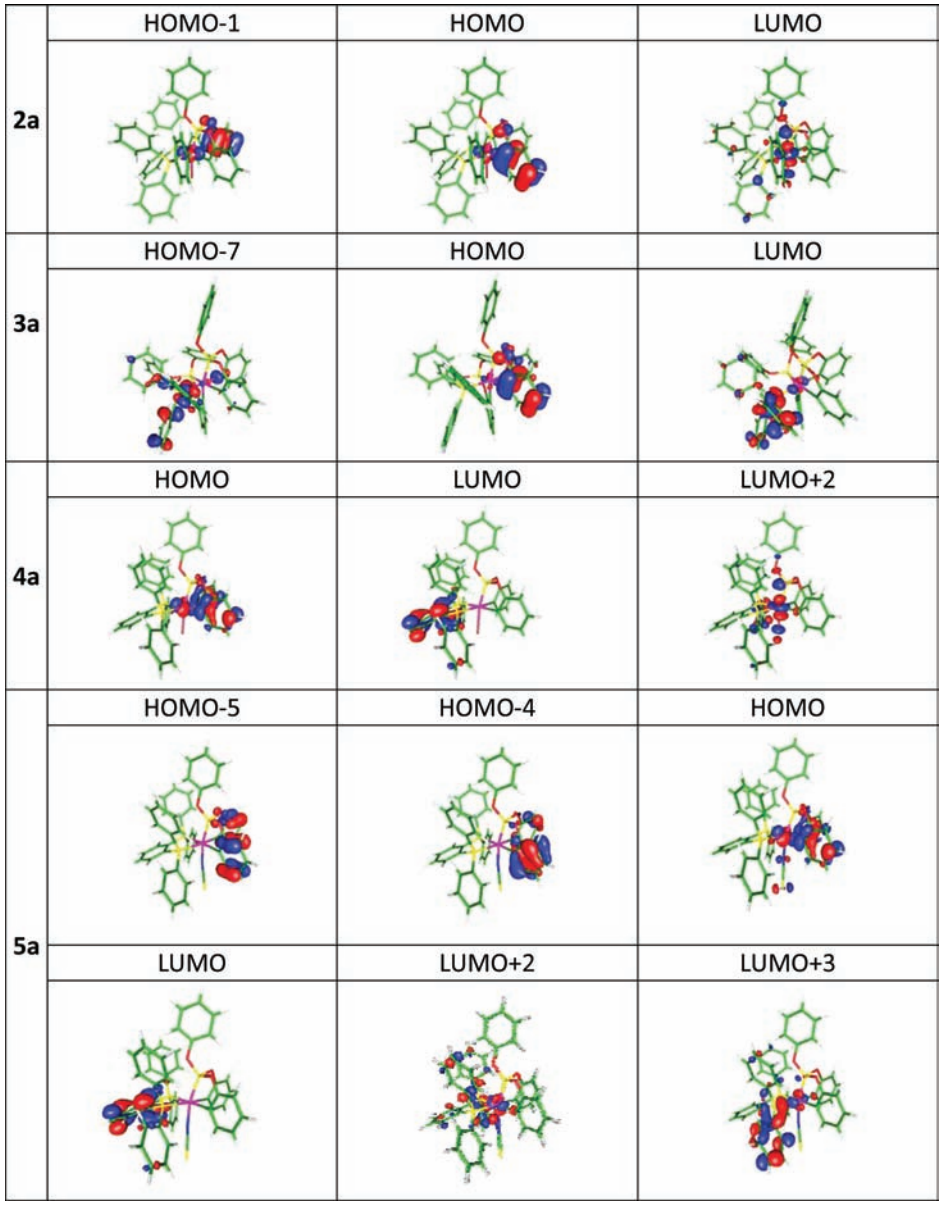

Figure 9. Selected frontier orbitals involved in the lower-lying transition for **2a**−**5a**.

2a−**c**, **3a**, and **6c**), except for those involving the dppb chelate (c.f. **4a**−**b** and **5a**−**b**), where LUMO is mainly localized on the dppb π^* orbital, due to the lower gap of *o*-phenylene fragment versus that of phenyl groups of triphenylphosphite. Nevertheless, other higher lying orbitals such as LUMO+1 to LUMO +3, which are also involved in the T_1 state, still have substantial contribution from the d_{σ^*} orbital. Evidently, all Ir(III) complexes show dominant MC *dd* character in their T_1 excited state according to the aforementioned argument.

In contrast to the above approach, which is based on a full geometry optimization for an isolated complex surrounded by solvent molecules that mimic the diluted solution, the X-ray structural data were also taken to perform the TDDFT calculation to simulate the respective electronic properties in solid state. Again, all results showed significant *dd* contribution in the T_1 excited state (see Figure S1 of the Supporting Information). This can be confirmed by the Mulliken population analysis,[28] in which the net spin value is located mainly on the Ir(III) metal atom. Therefore, for all titled complexes the T_1 state possesses a significant amount of ^{3}MC *dd* character; its repulsive PES, in theory, touches the ground-state dissociation level, greatly facilitating the radiationless deactivation or even weakening the metal−ligand bonds. Such deactivation process is virtually barrierless and requires no thermal activation, rationalizing the lack of emission even in the 77 K CH_2Cl_2 matrix.

Electrochemistry. The electrochemical behavior of these Ir(III) metal complexes was investigated by cyclic voltammetry as supplement to that obtained by spectroscopic and theoretical measurements. These redox data are listed in Table 3. It is notable that all electrochemical processes are irreversible which is in good agreement with the higher absorption onset in the UV/vis spectra and the larger energy gaps obtained in DFT calculation. Despite their irreversibility, we can still extract certain systematic trends, such as the reduction of the gap between oxidation and reduction peak potentials for the tripodal substituted phosphonite complexes **2b** and **4b** versus that of phosphite complexes **2a** and **4a**, which could be due to

dx.doi.org/10.1021/ic202090j | *Inorg. Chem.* 2012, 51, 1785−1795

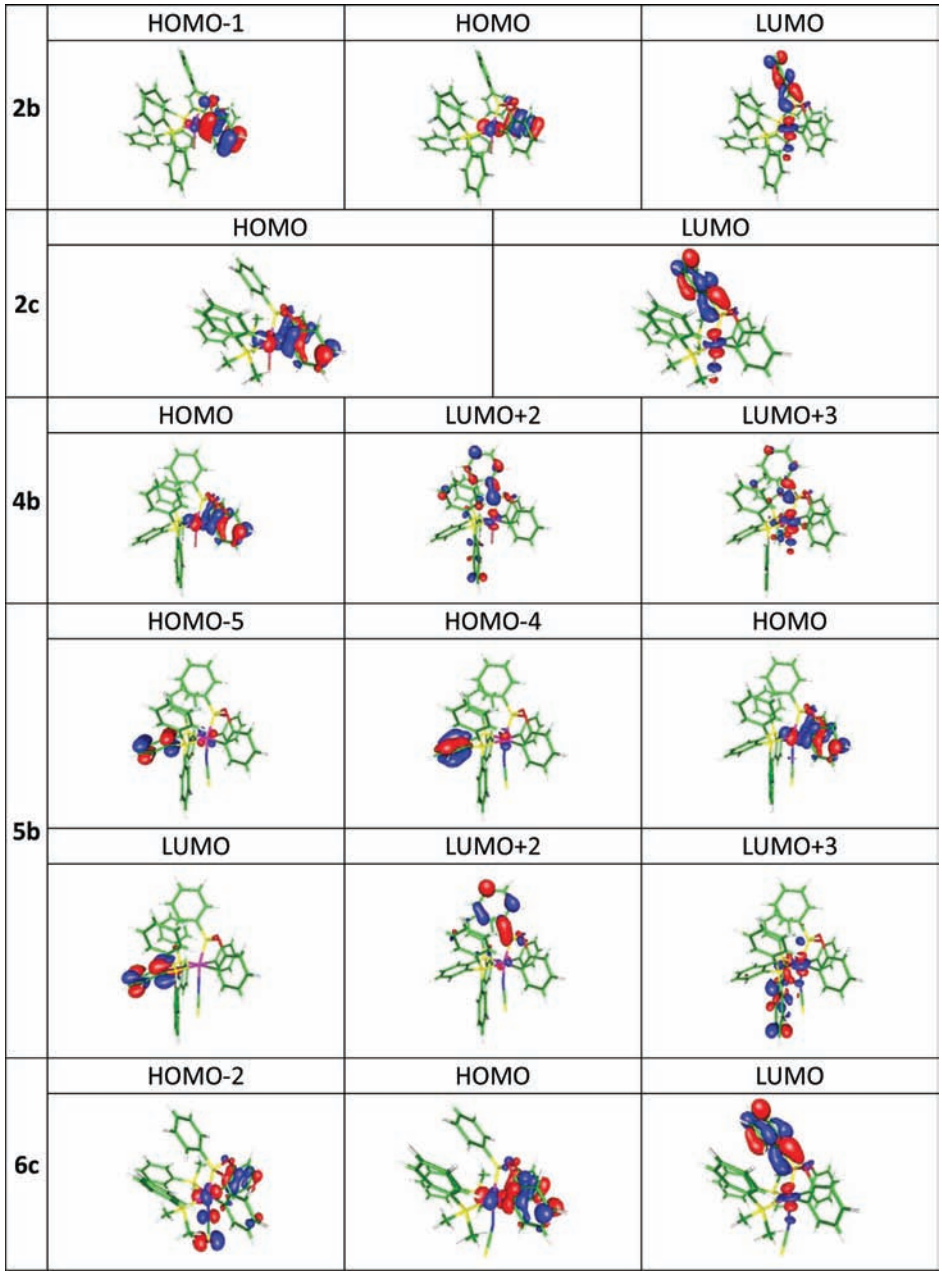

Figure 10. Selected frontier orbitals involved in the lower-lying transition for **2b**−**6c**.

the increased contribution of phenyl substituent of phosphonite to the frontier orbitals. Furthermore, the thiocyanate complexes **5b** and **6c** show more positive oxidization peak potential versus that of the chloride counterparts **4b** and **2c**. This could be attributed to the relative poor π-donating property of the thiocyanate ligand.[26c]

4. CONCLUSION

In sum, this study demonstrates the successful synthesis of a series of Ir(III) complexes with phosphite (or phosphonite) tripodal dicyclometalates. It appears that, in presence of two equiv of PPh_3, cyclometalation of phosphite (or phosphonite) proceeds in a stepwise fashion, for which the first product, c.f. $[Ir(tpitH)(PPh_3)_2Cl_2]$ (**1a**), shows a monocyclometalated phosphite, with two PPh_3 and two chlorides occupying mutual trans and cis disposition. Further cyclometalation is concomitantly accompanied with trans-to-cis isomerization of PPh_3 and detachment of one chloride, giving the tripodal coordinated Ir(III) complex $[Ir(tpit)(PPh_3)_2Cl]$ (**2a**) in high yield, as the representative example. Subsequent replacement of PPh_3 and PMe_2Ph with chelating diphosphine and substitution of chloride with thiocyanate are both feasible. Of particular interest is the introduction of a second triphenylphosphite on **2a**, which gives formation of $[Ir(tpit)(tpitH)(PPh_3)]$ (**3a**) with all types of tripodal, bidentate, and monodentate phosphorus donors coexisting on the Ir(III) coordination sphere. Due to the lack of largely extended and/or heterocyclic $\pi\pi^*$ chromophores for these Ir(III) complexes, the ^{3}MC *dd* transition seems to be substantially incorporated into the T_1 excited state. The repulsive PES of the resulting ^{3}MC *dd* state, in theory, should touch the PES of the ground state S_0, giving the dominant radiationless deactivation and hence virtually no emission under all conditions.

dx.doi.org/10.1021/ic202090j | *Inorg. Chem.* 2012, 51, 1785−1795

Table 2. Computational Energy Levels, Oscillator Strengths, and Orbital Transition Analyses at S_1 and T_1 for 2a–6c

		λ_{cal}	f	assignment
2a	S_1	337.0	0.0012	HOMO → LUMO (43%)
				HOMO-1 →LUMO (35%)
	T_1	353.0	0.0000	HOMO → LUMO (52%)
				HOMO-1 → LUMO (17%)
3a	S_1	330.7	0.0566	HOMO → LUMO (69%)
				HOMO-2 → LUMO (5%)
	T_1	342.6	0.0000	HOMO-7 → LUMO (80%)
				HOMO-7 → LUMO+2 (6%)
4a	S_1	336.6	0.0167	HOMO → LUMO+2 (69%)
				HOMO → LUMO (11%)
	T_1	350.9	0.0000	HOMO → LUMO+2 (50%)
				HOMO → LUMO+6 (5%)
5a	S_1	334.8	0.0006	HOMO → LUMO (90%)
	T_1	346.4	0.0000	HOMO-5 → LUMO+2 (23%)
				HOMO-4 → LUMO+3 (14%)
				HOMO-8 → LUMO (9%)
2b	S_1	362.3	0.0008	HOMO → LUMO (78%)
				HOMO-1 → LUMO (12%)
	T_1	395.2	0.0000	HOMO → LUMO (71%)
				HOMO-1 → LUMO (11%)
2c	S_1	348.7	0.0005	HOMO → LUMO (91%)
	T_1	376.4	0.0000	HOMO → LUMO (82%)
				HOMO-1 → LUMO+6 (6%)
4b	S_1	338.5	0.0202	HOMO → LUMO+3 (48%)
				HOMO → LUMO+2 (33%)
				HOMO → LUMO+1 (5%)
	T_1	365.8	0.0000	HOMO → LUMO+3 (67%)
				HOMO → LUMO+2 (12%)
				HOMO → LUMO+7 (7%)
5b	S_1	337.3	0.0001	HOMO → LUMO (90%)
	T_1	346.1	0.0000	HOMO-5 → LUMO+3 (33%)
				HOMO-4 → LUMO+2 (21%)
				HOMO-7 → LUMO (7%)
6c	S_1	320.8	0.0014	HOMO → LUMO (93%)
	T_1	343.4	0.0000	HOMO-2 → LUMO (22%)
				HOMO-1 → LUMO (15%)
				HOMO → LUMO (15%)

Table 3. Electrochemical Data of Ir (III) Complexes 2a–6c[a]

complex	E_{pa}^{ox}	E_{pc}^{red}
2a	0.939	−2.936
2b	0.841	−2.598
2c	0.923	−2.582
3a	0.958	−2.155
4a	0.920	−2.707
4b	0.814	−2.627
5a	0.989	−2.667
5b	0.936	−2.566
6c	1.017	−2.567

[a]The oxidation and reduction experiments were conducted in CH_2Cl_2 and THF solution, respectively; E_{pa} and E_{pc} are the anodic and cathodic peak potentials referenced to the Fc^+/Fc couple in V.

■ ASSOCIATED CONTENT

Supporting Information

Cyclic voltammogram and X-ray crystallographic data file (CIF) of all studied complexes. This material is available free of charge via the Internet at http://pubs.acs.org.

■ AUTHOR INFORMATION

Corresponding Author

*E-mail: ychi@mx.nthu.edu.tw (Y.C.), chop@ntu.edu.tw (P.-T.C.).

■ ACKNOWLEDGMENTS

This work was supported by the National Science Council and Ministry of Economy of Taiwan, project 100-EC-17-A-08-S1-042. We are also grateful to the National Center for High-Performance Computing for computer time and facilities.

■ DEDICATION

†Dedicated to Dr. Hubert Le Bozec on the occasion of his 60th birthday.

■ REFERENCES

(1) (a) Yoon, T. P.; Ischay, M. A.; Du, J. *Nat. Chem.* **2010**, *2*, 527. (b) Pettinari, C.; Masciocchi, N.; Pandolfo, L.; Pucci, D. *Chem.—Eur. J.* **2010**, *16*, 1106. (c) Ward, M. D. *Dalton Trans.* **2010**, *39*, 8551. (d) Hudson, Z. M.; Wang, S. *Acc. Chem. Res.* **2009**, *42*, 1584. (e) Sakai, K.; Ozawa, H. *Coord. Chem. Rev.* **2007**, *251*, 2753. (f) Marin, V.; Holder, E.; Hoogenboom, R.; Schubert, U. S. *Chem. Soc. Rev.* **2007**, *36*, 618. (g) Maury, O.; Bozec, H. Le *Acc. Chem. Res.* **2005**, *38*, 691. (h) Hissler, M.; McGarrah, J. E.; Connick, W. B.; Geiger, D. K.; Cummings, S. D.; Eisenberg, R. *Coord. Chem. Rev.* **2000**, *208*, 115. (i) Stufkens, D. J.; Vlcek, A. Jr. *Coord. Chem. Rev.* **1998**, *177*, 127.

(2) (a) Zhou, G.; Wong, W.-Y.; Yang, X. *Chem. Asian J.* **2011**, *6*, 1706. (b) Chi, Y.; Chou, P.-T. *Chem. Soc. Rev.* **2010**, *39*, 638. (c) You, Y.; Park, S. Y. *Dalton Trans.* **2009**, 1267. (d) Chou, P.-T.; Chi, Y. *Chem.—Eur. J.* **2007**, *13*, 380. (e) Evans, R. C.; Douglas, P.; Winscom, C. J. *Coord. Chem. Rev.* **2006**, *250*, 2093. (f) Zhou, G.; Wong, W.-Y.; Suo, S. *J. Photochem. Photobiol. C* **2010**, *11*, 133.

(3) (a) Williams, J. A. G. *Chem. Soc. Rev.* **2009**, *38*, 1783. (b) Henderson, W. *Adv. Organomet. Chem.* **2006**, *54*, 207. (c) Slagt, M. Q.; van Zwieten, D. A. P.; Moerkerk, A. J. C. M.; Gebbink, R. J. M. K.; van Koten, G. *Coord. Chem. Rev.* **2004**, *248*, 2275. (d) Steenwinkel, P.; Gossage, R. A.; van Koten, G. *Chem.—Eur. J.* **1998**, *4*, 759. (e) Wong, W.-Y.; Ho, C.-L. *Coord. Chem. Rev.* **2009**, *253*, 1709. (f) Wong, W.-Y.; Ho, C.-L. *J. Mater. Chem.* **2009**, *19*, 4457.

(4) (a) Ryabov, A. D. *Chem. Rev.* **1990**, *90*, 403. (b) Shilov, A. E.; Shul'pin, G. B. *Chem. Rev.* **1997**, *97*, 2879. (c) Werner, H. *Dalton Trans.* **2003**, 3829. (d) Omae, I. Coord. *Chem. Rev.* **2004**, *248*, 995. (e) Albrecht, M. *Chem. Rev.* **2010**, *110*, 576.

(5) (a) Hiraki, K.; Fuchita, Y.; Uchiyama, T. *Inorg. Chim. Acta* **1983**, *69*, 187. (b) Muller, G.; Abicht, H.-P.; Waldkircher, M.; Lachmann, J.; Lutz, M.; Winkler, M. *J. Organomet. Chem.* **2001**, *622*, 121. (c) Bedford, R. B.; Hazelwood, S. L.; Horton, P. N.; Hursthouse, M. B. *Dalton Trans.* **2003**, 4164. (d) Mohr, F.; Priver, S. H.; Bhargava, S. K.; Bennett, M. A. *Coord. Chem. Rev.* **2006**, *250*, 1851. (e) Djukic, J.-P.; Sortais, J.-B.; Barloy, L.; Pfeffer, M. *Eur. J. Inorg. Chem.* **2009**, 817.

(6) Song, Y.-H.; Chiu, Y.-C.; Chi, Y.; Cheng, Y.-M.; Lai, C.-H.; Chou, P.-T.; Wong, K.-T.; Tsai, M.-H.; Wu, C.-C. *Chem.—Eur. J.* **2008**, *14*, 5423.

(7) (a) Chiu, Y.-C.; Hung, J.-Y.; Chi, Y.; Chen, C.-C.; Chang, C.-H.; Wu, C.-C.; Cheng, Y.-M.; Yu, Y.-C.; Lee, G.-H.; Chou, P.-T. *Adv. Mater.* **2009**, *21*, 2221. (b) Hung, J.-Y.; Chi, Y.; Pai, I.-H.; Cheng, Y.-M.; Yu, Y.-C.; Lee, G.-H.; Chou, P.-T.; Wong, K.-T.; Chen, C.-C.; Wu, C.-C. *Dalton Trans.* **2009**, 6472. (c) Hung, J.-Y.; Lin, C.-H.; Chi, Y.; Chung, M.-W.; Chen, Y.-J.; Lee, G.-H.; Chou, P.-T.; Chen, C.-C.; Wu, C.-C. *J. Mater. Chem.* **2010**, *20*, 7682. (d) Fu, H.; Cheng, Y.-M.; Chou, P.-T.; Chi, Y. *Mater. Today* **2011**, *14*, 472.

(8) (a) van der Boom, M. E.; Milstein, D. *Chem. Rev.* **2003**, *103*, 1759. (b) Goettker-Schnetmann, I.; Brookhart, M. *J. Am. Chem. Soc.* **2004**, *126*, 9330. (c) Baber, R. A.; Bedford, R. B.; Betham, M.; Blake, M. E.; Coles, S. J.; Haddow, M. F.; Hursthouse, M. B.; Orpen, A. G.; Pilarski, L. T.; Pringle, P. G.; Wingad, R. L. *Chem. Commun.* **2006**, 3880. (d) Fey, N.; Harvey, J. N.; Lloyd-Jones, G. C.; Murray, P.;

Orpen, A. G.; Osborne, R.; Purdie, M. *Organometallics* **2008**, *27*, 1372. (e) Salem, H.; Shimon, L. J. W.; Diskin-Posner, Y.; Leitus, G.; Ben-David, Y.; Milstein, D. *Organometallics* **2009**, *28*, 4791.
(9) Kuroda, K.; Maruyama, Y.; Hayashi, Y.; Mukaiyama, T. B. *Chem. Soc. Jpn.* **2009**, *82*, 381.
(10) Chiu, Y.-C.; Lin, C.-H.; Hung, J.-Y.; Chi, Y.; Cheng, Y.-M.; Wang, K.-W.; Chung, M.-W.; Lee, G.-H.; Chou, P.-T. *Inorg. Chem.* **2009**, *48*, 8164.
(11) Chou, P.-T.; Yu, W.-S.; Cheng, Y.-M.; Pu, S.-C.; Yu, Y.-C.; Lin, Y.-C.; Huang, C.-H.; Chen, C.-T. *J. Phys. Chem. A* **2004**, *108*, 6487.
(12) (a) Lee, C.; Yang, W.; Parr, R. G. *Phys. Rev. B* **1988**, *37*, 785. (b) Becke, A. D. *J. Chem. Phys.* **1993**, *98*, 5648.
(13) (a) Hay, P. J.; Wadt, W. R. *J. Chem. Phys.* **1985**, *82*, 270. (b) Hay, P. J.; Wadt, W. R. *J. Chem. Phys.* **1985**, *82*, 284. (c) Hay, P. J.; Wadt, W. R. *J. Chem. Phys.* **1985**, *82*, 299.
(14) Hariharan, P. C.; Pople, J. A. *Mol. Phys.* **1974**, *27*, 209.
(15) (a) Jamorski, C.; Casida, M. E.; Salahub, D. R. *J. Chem. Phys.* **1996**, *104*, 5134. (b) Petersilka, M.; Grossmann, U. J.; Gross, E. K. U. *Phys. Rev. Lett.* **1996**, *76*, 1212. (c) Bauernschmitt, R.; Ahlrichs, R.; Hennrich, F. H.; Kappes, M. M. *J. Am. Chem. Soc.* **1998**, *120*, 5052. (d) Casida, M. E. *J. Chem. Phys.* **1998**, *108*, 4439. (e) Stratmann, R. E.; Scuseria, G. E.; Frisch, M. J. *J. Chem. Phys.* **1998**, *109*, 8218.
(16) Cancès, M. T.; Mennucci, B.; Tomasi, J. *J. Chem. Phys.* **1997**, *107*, 3032.
(17) Frisch, M. J.; et al. *Gaussian 03*, revision C.02; Gaussian, Inc.: Wallingford, CT, 2004.
(18) Chang, Y.-Y.; Hung, J.-Y.; Chi, Y.; Chyn, J.-P.; Chung, M.-W.; Lin, C.-L.; Chou, P.-T.; Lee, G.-H.; Chang, C.-H.; Lin, W.-C. *Inorg. Chem.* **2011**, *50*, 5075.
(19) Lin, C.-H.; Chang, Y.-Y.; Hung, J.-Y.; Lin, C.-Y.; Chi, Y.; Chung, M.-W.; Lin, C.-L.; Chou, P.-T.; Lee, G.-H.; Chang, C.-H.; Lin, W.-C. *Angew. Chem., Int. Ed.* **2011**, *50*, 3182.
(20) (a) Singleton, E.; Van der Stok, E. *J. Chem. Soc., Dalton Trans.* **1978**, 926. (b) Bedford, R. B.; Chaloner, P. A.; Hitchcock, P. B. *J. Chem. Soc. Chem. Commun.* **1995**, 2049. (c) Bedford, R. B.; Castillon, S.; Chaloner, P. A.; Claver, C.; Fernandez, E.; Hitchcock, P. B.; Ruiz, A. *Organometallics* **1996**, *15*, 3990.
(21) (a) Lee, C.-L.; Das, R. R.; Kim, J.-J. *Chem. Mater.* **2004**, *16*, 4642. (b) Lyu, Y.-Y.; Byun, Y.; Kwon, O.; Han, E.; Jeon, W. S.; Das, R. R.; Char, K. *J. Phys. Chem. B* **2006**, *110*, 10303. (c) Du, B.-S.; Lin, C.-H.; Chi, Y.; Hung, J.-Y.; Chung, M.-W.; Lin, T.-Y.; Lee, G.-H.; Wong, K.-T.; Chou, P.-T.; Hung, W.-Y.; Chiu, H.-C. *Inorg. Chem.* **2010**, *49*, 8713. (d) Lin, C.-H.; Chi, Y.; Chung, M.-W.; Chen, Y.-J.; Wang, K.-W.; Lee, G.-H.; Chou, P.-T.; Hung, W.-Y.; Chiu, H.-C. *Dalton Trans.* **2011**, *40*, 1132.
(22) Nolte, M. J.; Singleton, E.; Van der Stok, E. *J. Organomet. Chem.* **1977**, *142*, 387.
(23) Poë, A. J. *Dalton Trans.* **2009**, 1999 and references cited therein.
(24) (a) Tamayo, A. B.; Alleyne, B. D.; Djurovich, P. I.; Lamansky, S.; Tsyba, I.; Ho, N. N.; Bau, R.; Thompson, M. E. *J. Am. Chem. Soc.* **2003**, *125*, 7377. (b) Sajoto, T.; Djurovich, P. I.; Tamayo, A.; Yousufuddin, M.; Bau, R.; Thompson, M. E.; Holmes, R. J.; Forrest, S. R. *Inorg. Chem.* **2005**, *44*, 7992. (c) Deaton, J. C.; Young, R. H.; Lenhard, J. R.; Rajeswaran, M.; Huo, S. *Inorg. Chem.* **2010**, *49*, 9151.
(25) (a) Chinchilla, R.; Najera, C. *Chem. Rev.* **2007**, *107*, 874. (b) Khairul, W. M.; Fox, M. A.; Zaitseva, N. N.; Gaudio, M.; Yufit, D. S.; Skelton, B. W.; White, A. H.; Howard, J. A. K.; Bruce, M. I.; Low, P. J. *Dalton Trans.* **2009**, 610.
(26) (a) Nazeeruddin, M. K.; Humphry-Baker, R.; Berner, D.; Rivier, S.; Zuppiroli, L.; Graetzel, M. *J. Am. Chem. Soc.* **2003**, *125*, 8790. (b) Chen, K.-S.; Liu, W.-H.; Wang, Y.-H.; Lai, C.-H.; Chou, P.-T.; Lee, G.-H.; Chen, K.; Chen, H.-Y.; Chi, Y.; Tung, F.-C. *Adv. Funct. Mater.* **2007**, *17*, 2964. (c) Shen, X.; Hu, X.-H.; Wang, F.-L.; Sun, F.; Yang, Y.-Q.; Xu, Y.; Chen, S.; Zhu, D.-R. *Inorg. Chem. Commun.* **2010**, *13*, 1096.
(27) Chou, P.-T.; Chi, Y.; Chung, M.-W.; Lin, C.-C. *Coord. Chem. Rev.* **2011**, *255*, 2653.
(28) (a) Mulliken, R. S. *J. Phys. Chem.* **1955**, *23*, 1833. (b) Bickelhaupt, F. M.; van Eikema Hommes, N. J. R.; Fonseca Guerra, C.; Baerends, E. J. *Organometallics* **1996**, *15*, 2923.